AMPTIAC

A Facsimile Report

Reproduced by

UNITED STATES
ATOMIC ENERGY COMMISSION

Division of Technical Information
P.O. Box 62   Oak Ridge, Tennessee   37830

DTIC QUALITY INSPECTED 4

20000907 193

UCRL-17445

T6269

61

UCRL

17449

UNIVERSITY OF CALIFORNIA

Lawrence Radiation Laboratory
Berkeley, California

THE LOW TEMPERATURE THERMALLY ACTIVATED DEFORMATION MECHANISMS FOR BCC MAGNESIUM-LITHIUM-ALUMINUM ALLOY

Mohamed Osama Abo-el-Fotch

(M.S. thesis)

March 1967

Contents

THE LOW TEMPERATURE THERMALLY ACTIVATED DEFORMATION MECHANISMS FOR BCC MAGNESIUM-LITHIUM-ALUMINUM ALLOY

Contents

I. INTRODUCTION

This investigation was undertaken for the purpose of elucidating

the rate-controlling mechanism for slip in polycrystalline aggregates

of b.c.c. magnesium, 14 wt.% Li, 1.0 - 1.5 wt.% Al alloy as part of a

more general program of study on the plastic behavior of b.c.c. metals,

alloys, and intermetallic compounds. The flow stress of this alloy

depends strongly on temperature and strain rate over the low temperature

region (below about 115°K). A basic understanding of its mechanical

behavior necessitates a thorough investigation of the rate controlling

mechanisms of the mobile dislocations. The following thermally-activated

dislocation mechanisms have been proposed:

(a) Interaction of dislocations with interstitial
impurity atoms or with solute atoms in general,

(b) Overcoming the Peierls-Nabarro stress,

(c) Resistance to the motion of dislocations due to jogs
on screw dislocations,

(d) Overcoming interstitial precipitates,

(e) Cross-slip.

It was concluded by Dorn and Rajnak,[1] Conrad,[2] and Christian and

Masters,[3] that in b.c.c. metals the overcoming of the Peierls-Nabarro

stress which arises from the variations in bond energies of atoms in the

dislocation core as it is displaced, is the most probable rate controlling

mechanism. Several models of the Peierls mechanism have been formulated.

Experimental results obtained from the deformation of Mo, Nb, Ta, AgMg,

AuZn and Fe-2 % Mn alloy have been successfully explained by the Dorn-

Rajnak model of nucleation of kink pairs.

THE LOW TEMPERATURE THERMALLY ACTIVATED DEFORMATION MECHANISMS
FOR BCC MAGNESIUM-LITHIUM-ALUMINUM ALLOY

Mohamed Osama Abo-el-Fotoh

Inorganic Materials Research Division, Lawrence Radiation Laboratory,
and Department of Mineral Technology, College of Engineering,
University of California, Berkeley, California

March, 1967

ABSTRACT

The effect of strain rate and temperature on the flow stress was

investigated in a polycrystalline magnesium-14 wt.% lithium-1.5 wt.%

aluminum alloy. Whereas the flow stress increased only slightly as the

temperature was decreased from room temperature to about 115°K, a rapid

increase in the flow stress was obtained with yet greater decreases

in temperature from about 115° to 20°K. The strong temperature and

strain rate dependence of the flow stress below 115°K was interpreted

in terms of the Dorn-Rajnak theory of the Peierls mechanism when the

deformation is controlled by the rate of nucleation of pairs of kinks.

Above 115°K, an athermal mechanism is operative.

Start

The purpose of this work was to investigate the mechanical behavior of polycrystalline aggregates of magnesium, 14 wt.% Li, and 1.0 - 1.55 Å alloy at low temperatures and to correlate the experimental results with the Peierls mechanism using the Dorn and Rajnak model.

It will be shown that the strong dependence of temperature and strain rate can be satisfactorily explained by the rate of nucleation of pairs of kinks on dislocations involved in the Peierls mechanism for plastic deformation.

1 to p. V

II. DORN AND RAJNAK'S MODEL OF PEIERLS' MECHANISM

A straight dislocation line has its lowest energy when it lies in a potential valley parallel to lines of closest packing of atoms on the slip plane. When such a straight dislocation line moves from one valley toward the next, the atoms in the vicinity of the core of the dislocation change their positions and bond angles, causing the energy of the dislocation to increase. The core energy of the dislocation is assumed to reach a maximum value midway between the two adjacent valleys. Any additional small displacement will cause the dislocation to fall down the hill into the next valley which is another minimum energy position for the dislocation. The shear stress necessary to promote such forward motion of the dislocation at the absolute zero is known as the Peierls stress τ_p.

A forward motion of such kind can be achieved by the nucleation of a pair of kinks under the influence of an applied stress and a thermal fluctuation. When a stress τ* less than τ_p is applied to the slip plane in the direction of the Burger's vector, the dislocation will move as shown in Fig. 1, from its original position $A_0B_0C_0$ in the valley to a parallel position ABC part way up the Peierls hill. No further motion will occur at the absolute zero. At higher temperatures, thermal fluctuations cause the dislocation to vibrate about its mean position. When a local thermal fluctuation is sufficiently energetic, a dislocation loop AB'C of a critical size is produced which no longer returns to its original position. For all configurations exceeding the critical one, the two kink segments AB' and B'C will move apart under the action of the applied stress, resulting in a forward motion of the dislocation by a displacement,

---

b, equal to the periodicity of the rows of closely spaced atoms on the slip plane.

Dorn and Rajnak applied the suggestion of Friedel that the major factor involved in kink nucleation is the additional energy due to the increase in the length of the dislocation line. Γ_y was taken to be the energy per unit length of a dislocation where the y direction was defined as shown in Fig. 1. Therefore, the line energy was assumed to be a periodic function of y with a period a. The minor variations of the line energy with curvature and proportions of edge and screw dislocations were neglected. Furthermore, although the exact shape of the Peierls hill was not known, it was assumed by Dorn and Rajnak to be approximated by:

$$\Gamma_{(y)} = \frac{\Gamma_i + \Gamma_o}{2} + \frac{\Gamma_i - \Gamma_o}{2}\left(\frac{a}{2} + \cos\frac{2\pi y}{a} - \frac{a}{4}\cos\frac{4\pi y}{a}\right) \quad (1)$$

where Γ_i and Γ_o are the energies per unit length of a dislocation lying at the top and bottom of the Peierls hill, respectively, and α is a hill shape factor that was assumed to vary between -1 and $+1$.

Under a stress τ^* the stable equilibrium position of an infinitely long dislocation is y = y_o. The difference in energy of a displaced dislocation line (ABC, Fig. 1) and that of the corresponding straight dislocation line lying along y = y_o is given by

$$U = \int_{-\infty}^{\infty}\left\{\Gamma_{(y)}\sqrt{1+\left(\frac{dy}{dx}\right)^2} - \Gamma_{(y_o)} - \tau^* b(y-y_o)\right\}dx \quad (2)$$

where the first two terms of the integrand are the line energies of the

dislocation in the two positions, and the third term gives the extra work done by the applied stress τ^* in displacing the dislocation from y_o to y.

The critical energy for nucleating one pair of kinks was calculated by using Euler's conditions for minimizing the energy. Upon numerical integration of the above equations, Dorn and Rajnak were able to obtain a universal relationship between $U_n/2U_k$ and τ^*/τ_p (U_k is the kink energy), from which relationship could be derived between the activation volume and the applied stress, and between the velocity of the dislocation and the applied stress.

UCRL-17449

-4-   -5-

III. EXPERIMENTAL PROCEDURE

The material used in this investigation consisted of a b.c.c. magnesium, Li ... Al alloy. Tensile specimens 0.2" in dia having 2" long gauge section were machined from the as received 1 in x 6 in x 12 in sheets, annealed under argon at 300°F (=150°C) for 4 hours to remove all the deformation put into the specimen during the machining and finally etched in dilute hydrochloric acid solution to remove the thin oxide films.

The tensile tests were performed at strain rates of 3.13×10^{-3} sec^{-1} and 3.13×10^{-5} sec^{-1} on an Instron testing machine in controlled temperature baths. The temperature variation was controlled within ±2°K of the recorded value. For testing temperatures below 77°C, a specially designed cryostat was used.

IV. EXPERIMENTAL RESULTS AND DISCUSSION

The dependence of flow stress on temperature and strain rate:

The applied shear stress that is required to cause plastic flow is given by:

$$\tau = \tau^* + \tau_A \qquad (3)$$

where τ is the applied shear stress, and τ^* is the stress required to aid the thermal activation of the rate controlling mechanism and therefore decreases precipitously as T increases. τ_A is the stress necessary to overcome any athermal barriers and therefore it decreases only modestly as the temperature increases, usually parallel to the shear modulus of elasticity.

The primary interests of this work lie in the temperature and strain rate dependence of the dependence of the thermally activated component of the stress. The results are shown in Fig. 2 and Fig. 3.

The increasing flow stress with increasing strain rate as well as decreasing temperature attests to the fact that the operative deformation mechanism is thermally activated. Tests below 20°K were not performed due to the difficulties in controlling the stability of temperature. The curves in Figs. 2 and 3 were extrapolated to 0°K. Over the lower ranges of test temperatures, where the flow stress decreases rapidly from 20°K to 1.5°K for both strain rates, the thermally activated component τ^* of the stress was calculated from the relationship:

$$\tau^* = \left(\tau_m - \tau_{35}\right) \frac{G(T)}{G(295)} \qquad (4)$$

-5-

where τ_μ is the total resolved shear stress for flow at temperature T°K, and the term $\tau_{235} \frac{G(T)}{G(235)}$ is the total back stress, corrected for the change in shear modulus with temperature. The variation of shear modulus with temperature was calculated from data obtained by J. Trivisonno and S. Smith, Fig. 4. Values of τ^*, which are now corrected for specimen variation in τ_μ, are shown in Fig. 3 for two strain rates.

For a thermally activated mechanism, the plastic strain rate is given by [see Appendix II]:

$$\dot{\gamma} = \frac{\rho L a b^2 \nu}{2w^2} \, e^{-\frac{U_n(\tau^*)}{kT}} \qquad (5)$$

where ρ = density of mobile dislocations

   a = the distance between Peierls' valleys

   b = Burger's vector

   ν = the Debye frequency

   L = the mean length swept out by a pair of kinks once nucleation occurs in that length

   w = width of a pair of kinks at the saddle point free energy configuration

   $U_n(\tau^*)$ = Saddle point free energy for nucleation of pairs of kinks

   K = Boltzmann constant

   T = absolute temperature

When the testing temperature reaches a critical temperature, T_c, for a given strain rate, the thermally activated component of the stress τ^* becomes zero and the thermal energy that needs to be supplied to nucleate

---

-9-

a pair of kinks is just $2U_K$, where U_K is the energy of a single kink. Therefore, at $T = T_c$

$$\dot{\gamma} = \frac{\rho L a b^2 \nu}{2w_c^2} \, e^{-\frac{2U_K(T_c)}{kT_c}} \qquad (6)$$

The theory of Dorn and Rajnak predicts a universal relationship between $U_n/2U_K$, where U_n is the saddle-point free energy for nucleation of a pair of kinks and U_K is the kink energy, and τ^*/τ_p. But as shown by Dorn and Rajnak, to a very good approximation $w \approx w_c$, where w_c is the critical width of a pair of kinks and therefore, as shown by Eqs. (5) and (6),

$$\frac{U_n(T)}{2U_K(T)} = \frac{U_n(T)}{2U_K(T_c)} \cdot \frac{G(T)}{G(T_c)} = \frac{\tau}{\tau_c} \cdot \frac{G(T_c)}{G(T)} \qquad (7)$$

It is the purpose of this work to correlate the relationship predicted by the theory with that obtained from the experimental results. The expected theoretical trends as shown by the solid curves in Fig. 5 are in excellent agreement with the experimental results at low temperatures (from 20°K to 115°K for $\dot{\gamma} = 3.13 \times 10^{-5}$ sec⁻¹ and from 20°K to 180°K for $\dot{\gamma}$ 3.13 × 10⁻³ sec⁻¹) and it appears to agree best with the curve representing $\alpha = +1$. At higher temperatures an athermal mechanism is operative. Experimental results are presented in Table 1.

-3-

V. ACTIVATION VOLUME

The activation volume is defined by:

$$V = -\left(\frac{\partial U}{\partial \tau^*}\right)_{\dot\epsilon} = kT\left(\frac{\partial \ln \dot\gamma}{\partial \tau^*}\right)_T = kT\left(\frac{\Delta \ln \dot\gamma}{\Delta \tau^*}\right)_T \quad (8)$$

The activation volume approximates the product of the Burger's vector and the area swept out during the nucleation of the critical loop (A'b'c', Fig. 14. The Peierls mechanism has a unique low value of the activation volume (usually ranging from 5b³ to 50b³). The activation volume remains constant and is unaffected by increasing the strain. These properties of the activation volume are the most reliable verification of the Peierls mechanism. The properties of the activation volume of the other suggested mechanisms are shown in Table 2. The experimental activation volumes are obtained by the effect of small changes in strain rate on the flow stress. A quantity β is defined as:

$$\beta = \left(\frac{\partial \ln \dot\gamma}{\partial \tau^*}\right)_T \quad (9)$$

βkT is defined as the apparent activation volume:

$$V_a = \beta kT = kT\left(\frac{\partial \ln \dot\gamma}{\partial \tau^*}\right)_T \quad (10)$$

For the Peierls mechanism (Eq. (5)), this becomes

$$V_a = kT\left(\frac{\partial \ln \rho}{\partial \tau^*}\right)_T - 2kT_w\left(\frac{\partial \ln w}{\partial \tau^*}\right)_T - \frac{\partial U_n}{\partial \tau^*} \quad (11)$$

Table 1. Strain rate, temperature dependence of the thermally activated component of the flow stress.

T°K	$\tau^* \times 10^{-8}$ dynes/cm²	
	$\dot\gamma = 3.13 \times 10^{-5}$ sec⁻¹	$\dot\gamma = 3.13 \times 10^{-3}$ sec⁻¹
10		6.71
20	5.97	
45		4.32
50	2.99	2.55
77	1.43	1.56
90	0.78	1.15
113	0.29	0.32
156	0	0
196	0	0
235	0	0.05
273	0.09	0.12
300	0	0.21

τ_p extrapolated = 8.40 × 10⁸ dynes/cm²

The critical temperature at $\dot\gamma_1 = 3.13 \times 10^{-5}$/sec. $T_{c1} = 115°K$

The critical temperature at $\dot\gamma_2 = 3.13 \times 10^{-3}$/sec. $T_{c2} = 180°K$

the negative of the last term of Eq. (11) is the theoretical activation volume V*. The theoretical activation volume V* can be rewritten as:

$$V^* = -\frac{\partial U_n}{\partial \tau^*} = -\frac{2U_k(C)}{\tau^\circ_p} \cdot \frac{\partial\left(\frac{U_n}{2U_k}\right)}{\partial\left(\frac{\tau^*}{\tau_p}\right)} \qquad (12)$$

Whereas the term containing w in Eq. (11) is always negligibly small, the apparent activation volume can be slightly larger than the theoretical one, v^*, as a result of the possible increase in the dislocation density, σ, as the stress is increased. Consequently, when the Peierls mechanism is operative, V_a closely follows the trends of v^*. Fig. 6 shows the apparent activation volume as a function of stress, the low values of V_a in terms of b^3 agree very well with the low activation volume as predicted by the Peierls mechanism. Figure 7 also shows the relatively constant value of the apparent activation volume with increasing strain. The theoretical plot for the activation volume as a function of $\frac{\tau^*}{\tau_p}$ for different values of α is shown in Fig. 5. The experimental values of $\frac{\tau^*}{\tau_p}$ for different values of $-\left(\frac{b}{2U_k}\right)\frac{\partial U}{\partial \tau^*}$ (corrected for change in shear modulus with temperature) are also plotted on the same figure, indicating the right order of magnitude of the experimental results.

Table 2. The properties of the activation volume of other suggested mechanisms.

Mechanism	Properties
Interaction of dislocations with interstitial impurity atoms or with solute atoms in general. [10-13]	1. V_a depends on interstitial content. Higher values of V_a (probably up to $1000b^3$).
Resistance to the motion of dislocations due to jogs on screw dislocations. [14-16]	1. V_a depends on the structure. 2. Athermal at low temperatures thermally activated at relatively high temperature. 3. $V_a = \ell_j b^2$ (ℓ_j = length of jog).
Overcoming interstitial precipitates. [17]	1. $V_a = \ell_i b^2$ (ℓ_i = length of the precipitates). 2. V_a varies with the impurity content.
Cross-slip. [18]	1. High activation volume (of the order of $700b^3 - 800b^3$).

VI. ACTIVATION ENERGY OF PAIRS OF KINKS

The apparent activation energy for nucleation of pairs of kinks is defined as:

$$U_K^* = \frac{\partial \ln \dot{\gamma}}{\partial \left(\frac{1}{kT}\right)_{\tau^*}} \tag{13}$$

The apparent activation energy for nucleation of pairs of kinks at 0°K can be determined by the change in strain rate due to the change in temperature at constant stress (τ^*).

$$\dot{\gamma} = \dot{\gamma}_o \, e^{-\frac{U_K}{kT}}$$

where:

$$\dot{\gamma}_o = \rho a b \frac{v}{2x^2}$$

At the critical temperature (where $\tau^* = 0$).

$$\dot{\gamma}_1 = \dot{\gamma}_o \, e^{-\frac{2U_K(T_{c1})}{kT_{c1}}}$$

$$\dot{\gamma}_2 = \dot{\gamma}_o \, e^{-\frac{2U_K(T_{c2})}{kT_{c2}}}$$

since $\dot{\gamma}_o$ remains constant for both cases,

$$\frac{\dot{\gamma}_2}{\dot{\gamma}_1} = \frac{\exp\left[-\frac{2U_K(T_{c2})}{kT_{c2}}\right]}{\exp\left[-\frac{2U_K(T_{c1})}{kT_{c1}}\right]} = \frac{\exp\left[-\frac{2U_K(0)}{kT_{c2}} \cdot \frac{G(T_{c2})}{G(0)}\right]}{\exp\left[-\frac{2U_K(0)}{kT_{c1}} \cdot \frac{G(T_{c1})}{G(0)}\right]}$$

or

$$2U_K(0) = \frac{kG(0) \ln\frac{\dot{\gamma}_2}{\dot{\gamma}_1}}{\frac{G(T_{c1})}{T_{c1}} - \frac{G(T_{c2})}{T_{c2}}} \tag{14}$$

Substituting:

$k = 1.38 \times 10^{-16}$ ergs/°K

$G(0) = 1.74 \times 10^{10}$ dynes/cm²

$G(T_{c1}) = 1.63 \times 10^{10}$ dynes/cm²

$G(T_{c2}) = 1.56 \times 10^{10}$ dynes/cm²

$T_{c1} = 115°K$

$T_{c2} = 180°K$

$$\ln\frac{\dot{\gamma}_2}{\dot{\gamma}_1} = 4.602$$

$$2U_K(0) = 0.2 \times 10^{-12}$$

$$= 2 \times 10^{-13} \text{ ergs} = 0.13 \text{ eV}$$

This value is of the right order of magnitude for activation energy, when the rate controlling mechanism is by nucleation of pairs of kinks.

IX. CONCLUSIONS

(1) The strong temperature dependence of the flow stress below ...sen can be explained by the Dorn and Rajnak theory of the Peierls mechanism of plastic deformation. Above about 115°K an athermal mechanism is operative.

(2) The shape of the Peierls hills for magnesium, 14 at.% Li, 2.5 ...% Li alloy seems to approach the theoretically predicted curve with α = 2.

(3) The activation energy of the process of the nucleation of pairs of kinks is estimated to be 0.13 eV, which is of the right order of magnitude for activation energy, when the rate-controlling mechanism is by nucleation of pairs of kinks.

(4) The experimentally deduced values of the apparent activation volume and the line tension are in agreement with the theory.

APPENDIX I

Various authors, Celli et al., [19] Friedel, [20] Gjssang et al., [21] Seeger et al., [22] have described the formulation of the forward velocity of dislocations and the strain rate resulting from the nucleation of pairs of kinks (see Brailsford (1961) regarding the redistribution of existing kinks along a dislocation due to the action of a stress). Only a first order approximation was attempted by P. Guyot and J. Dorn (1966).

L (Fig. 1) was assumed to be the average length of a dislocation that might be swept out by a pair of kinks following their nucleation. L was also assumed to be much larger than w, the width of the critical pair of kinks, and end effects were neglected. One possible formulation was based on the fact that there are 2/b (b is the Burger's vector) points along the length L at which a pair of kinks might be produced and consequently,

$$v_n = v_E \frac{L}{2b} e^{-\frac{U_n}{kT}}$$ (A.I.1)

where v_E is the Einstein frequency. This would apply for cases where the fluctuation might be localized. On the other hand when the thermal fluctuation is spread over the critical width, w, of the pair of kinks,

$$v_n' = \frac{vb}{w} \frac{L}{2w} e^{-\frac{U_n}{kT}}$$ (A.I.2)

where vb/w is the frequency of vibration of the dislocation, v is the Debye frequency, and $\frac{L}{2w}$ is approximately the number of wave lengths along the dislocation line at which nucleation might occur. These expressions

differs somewhat from the original suggestion of Dorn and Rajnak (1964) (which was based partly on both concepts) that

$$\nu_n = \frac{b}{x} \frac{\bar{L}}{b} \nu_D e^{-\frac{U_n}{kT}}$$ (A.I.3)

In what analysis for ν_n is quite complicated. Inasmuch as the vibrations are coupled, it appears that Eq. (A.I.2) might prove to be the more satisfactory approximation in most cases. These equations apply only when the velocity of the kinks is so great relative to their nucleation rate that not more than one pair of kinks exist in length L at any one time. Dorn and Rajnak (1964) have also described cases where the kink velocity might be so slow relative to the nucleation rate that several pairs of kinks will be moving along a single dislocation segment at one time. Thus far, however, there have been no experimental confirmations of this possibility.

The average velocity of a dislocation moving as a result of nucleation of pairs of kinks is

$$v = \nu_n a = \frac{\nu a b L}{2 x^2} e^{-\frac{U_n}{kT}}$$ (A.I.4)

and this gives a shear strain rate of

$$\dot{\gamma} = \rho b v = \frac{\rho L a b^2}{2 x^2} \nu e^{-\frac{U_n}{kT}}$$ (A.I.5)

where ρ is the total length of all thermally activatable dislocation segments per unit volume of the crystal.

ACKNOWLEDGMENT

REFERENCES

1. J. E. Dorn and S. Rajnak, Trans. AIME, 230, 1052 (1964).

2. H. Conrad, "Yielding and Flow of the BCC Metals at Low Temperature", Symposium on the Relation between Structure and Properties of Metals, National Physical Laboratory, Teddington, England (1962).

3. J. W. Christian and B. S. Masters, Proc. Roy. Soc., A, 281, 240 (1964).

4. A. Rosen and J. E. Dorn, Trans. AIME, 230, 1065 (1964).

5. P. Rumblett, A. Rosen and J. E. Dorn, Trans. AIME, 233, 652 (1965).

6. Pierre Guyot and J. E. Dorn, UCRL-16992, July, 1966.

7. Trinidonno and Charles S. Smith, Acta Met., 9 (12) Dec. (1961).

8. J. E. Dorn and J. B. Mitchell, High Strength Materials, Ed. V. Zackay, John Wiley and Sons, Inc., 510-77 (1965).

9. A. K. Mukherjee and J. E. Dorn, Trans. AIME, 230, 1065 (1964).

10. A. H. Cottrell, Rpt. on the Strength of Solids, Phys. Soc., London, 30 (1948); Conference on High Rates of Strain, Inst. Mech. Eng. London, p. 448.

11. A. H. Cottrell and B. A. Bilby, Proc. Phys. Soc., 62A, 49 (1949).

12. J. C. Fischer, Trans. ASM, 47, 451 (1955).

13. R. L. Jones, Proc. Phys. Soc., B69, 454 (1956); ibid. 371, 444 (1958).

14. G. Schoeck, Acta Met., 9, 382 (1961).

15. A. W. Rose, D. P. Ferris and J. Wulff, Trans. AIME, 224, 981 (1962).

16. B. L. Kordike, Zeit. f. Metall., 53, 586 (1962).

17. B. L. Kordike and P. Hassen, Phil. Mag., 7, 459 (1962).

18. B. L. Brown and R. A. Ekvall, Acta Met., 10, 1101 (1962).

19. H. Conrad, W. Kabler, T. Hinomiya and R. Thomson, Phys. Rev., 131,

58 (1963).

20. J. Friedel, NPL Conference, Teddington, England (1963); Dislocations, Pergamon Press (1964).

21. R. Gibberg, K. Skylsted, and J. Lothe, NPL Conference, Teddington, England (1963).

22. A. Seeger, H. Donth, and F. Pfaff, Discussion Faraday Soc., 23, 19 (1957).

23. R. Kossowsky and N. Brown, Technical Report of the University of Pennsylvania Laboratory for Research on the Structure of Matter, March 30, 1965.

24. S. Lau, private communication.

FIGURE CAPTIONS

Figure 1. Schematic diagram showing the nucleation of a pair of kinks. a is the spacing between parallel rows of closely spaced atoms of the slip plane.

Figure 2. 0.05% flow stress, τ, vs. temperature.

Figure 3. The thermally activated 0.05% flow stress, τ^*, vs. temperature.

Figure 4. Variation of shear modulus G with temperature.

Figure 5. The thermally activated component of the flow stress vs. temperature in dimensionless units.

Figure 6. The thermally activated component of the flow stress vs. the activation volume in units of b^3.

Figure 7. Apparent activation volume at 77°K vs. strain.

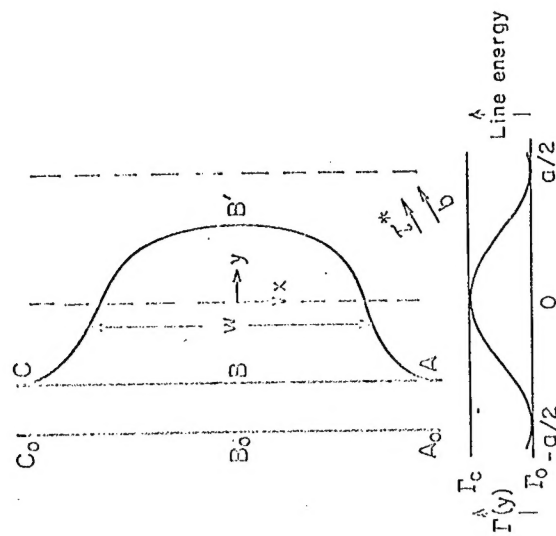Figure 8. The thermally activated component of the flow stress vs. activation volume in dimensionless units.
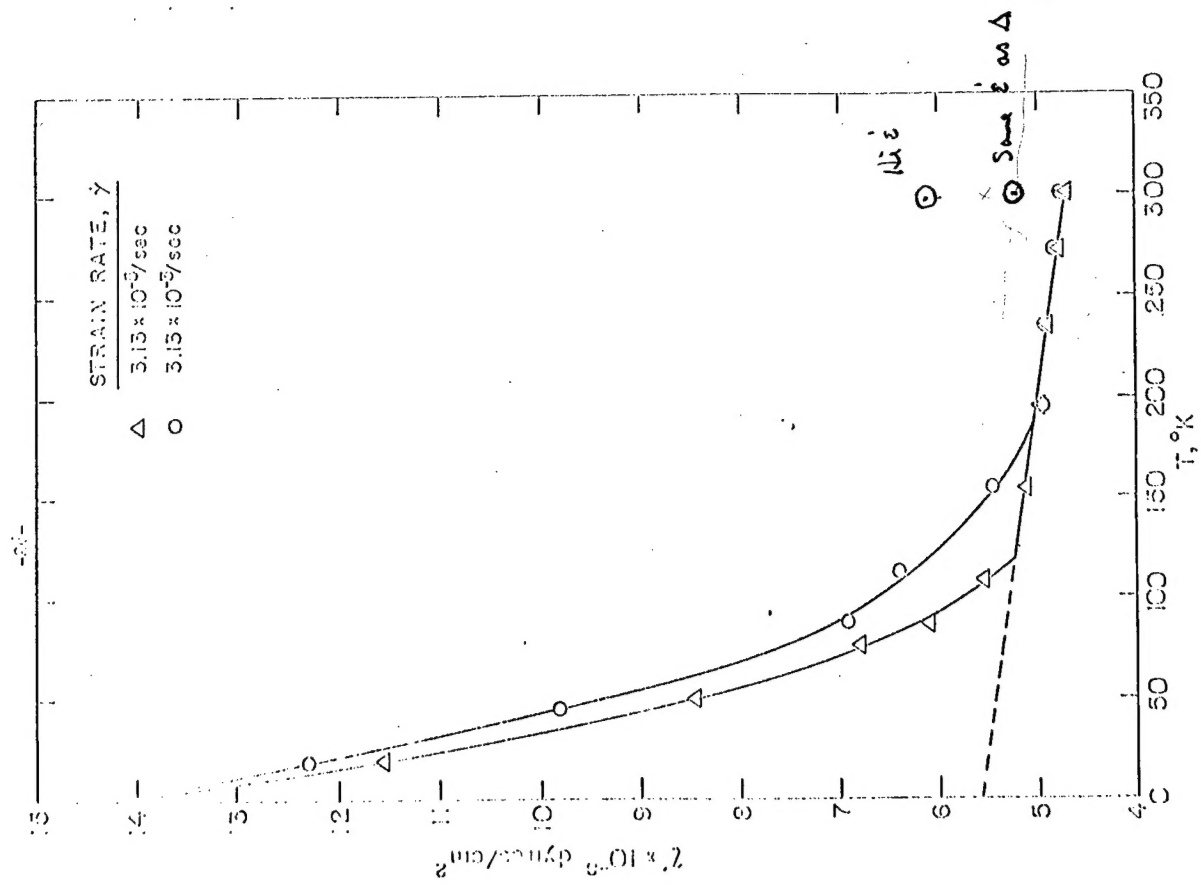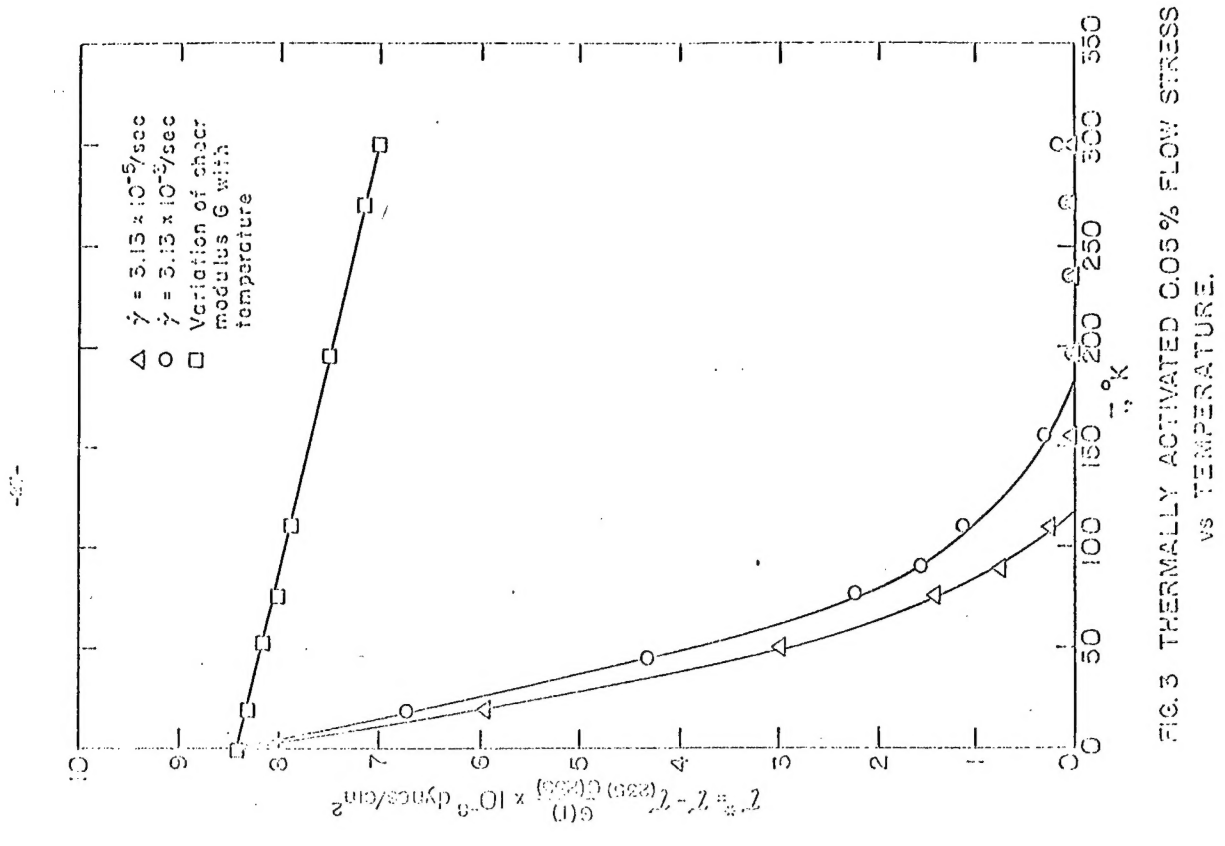

FIG. 1 NUCLEATION OF A PAIR OF KINKS.

FIG. 3

△ $\dot{\gamma} = 5.15 \times 10^{-5}$/sec
○ $\dot{\gamma} = 5.15 \times 10^{-3}$/sec
□ Variation of shear modulus G with temperature

$\tau^* = \tau - \tau^*_{(290)} \dfrac{G(T)}{G(290)} \times 10^{-8}$ dynes/cm²

T, °K

FIG. 3 THERMALLY ACTIVATED 0.05% FLOW STRESS vs TEMPERATURE.

STRAIN RATE, $\dot{\gamma}$

△ 5.15×10^{-5}/sec
○ 5.15×10^{-3}/sec

$\tau \times 10^{-8}$ dynes/cm²

T, °K

FIG. 2 0.05% FLOW STRESS vs TEMPERATURE.
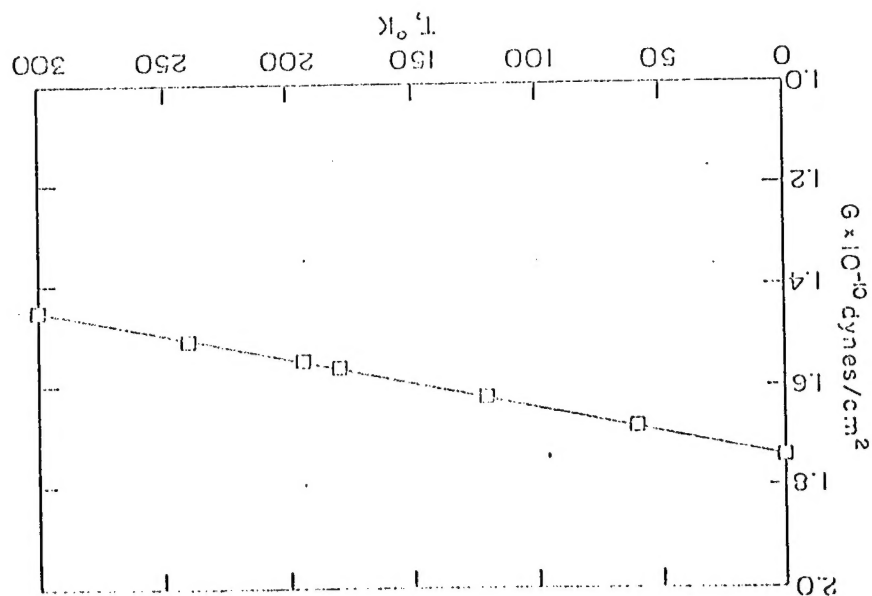
FIG. 5 THE THERMALLY ACTIVATED COMPONENT OF THE FLOW STRESS vs TEMPERATURE IN DIMENSIONLESS UNITS.

STRAIN RATE $\dot{\gamma}$

△ 5.15×10^{-5}/sec

○ 5.15×10^{-7}/sec

— · — $\alpha = -1$

——— $\alpha = 0$

— ·· — $\alpha = +1$

$\tau^*/\tau_p^0 \times G(0)/G\{T\}$

$U_m/2U_k = T/T_c \cdot G\{T_D\}/G\{T\}$

FIG.4 VARIATION OF SHEAR MODULUS G WITH TEMPERATURE.

$T, °K$

$G \times 10^{-10}$ dynes/cm^2